

AD _____

Award Number:
W81XWH-07-1-0039

TITLE:
Deregulated Wnt Signaling in Prostate Cancer

PRINCIPAL INVESTIGATOR:
Robin Tharakan, Ph.D.

CONTRACTING ORGANIZATION:
Fred Hutchinson Cancer Research Center
Seattle, WA 98109

REPORT DATE:
January, 2010

TYPE OF REPORT:

Final Report

PREPARED FOR: U.S. Army Medical Research and Materiel Command
Fort Detrick, Maryland 21702-5012

DISTRIBUTION STATEMENT:

x Approved for public release; distribution unlimited

The views, opinions and/or findings contained in this report are those of the author(s) and should not be construed as an official Department of the Army position, policy or decision unless so designated by other documentation.

REPORT DOCUMENTATION PAGE

Form Approved
OMB No. 0704-0188

Public reporting burden for this collection of information is estimated to average 1 hour per response, including the time for reviewing instructions, searching existing data sources, gathering and maintaining the data needed, and completing and reviewing this collection of information. Send comments regarding this burden estimate or any other aspect of this collection of information, including suggestions for reducing this burden to Department of Defense, Washington Headquarters Services, Directorate for Information Operations and Reports (0704-0188), 1215 Jefferson Davis Highway, Suite 1204, Arlington, VA 22202-4302. Respondents should be aware that notwithstanding any other provision of law, no person shall be subject to any penalty for failing to comply with a collection of information if it does not display a currently valid OMB control number. **PLEASE DO NOT RETURN YOUR FORM TO THE ABOVE ADDRESS.**

1. REPORT DATE (DD-MM-YYYY) 01-01-2010			2. REPORT TYPE Final Report			3. DATES COVERED (From - To) 01 Jan 2007 - 31 Dec 2009			
4. TITLE AND SUBTITLE Deregulated Wnt Signaling in Prostate Cancer						5a. CONTRACT NUMBER			
						5b. GRANT NUMBER W81XWH-07-1-0039			
						5c. PROGRAM ELEMENT NUMBER			
6. AUTHOR(S) Robin Tharakan, Ph.D.						5d. PROJECT NUMBER			
						5e. TASK NUMBER			
						5f. WORK UNIT NUMBER			
7. PERFORMING ORGANIZATION NAME(S) AND ADDRESS(ES) Fred Hutchinson Cancer Research Center, Seattle, WA 98109						8. PERFORMING ORGANIZATION REPORT NUMBER			
9. SPONSORING / MONITORING AGENCY NAME(S) AND ADDRESS(ES) US ARMY MEDICAL RESEARCH AND MATERIEL COMMAND FORT DETRICK, MARYLAND 21702-5012						10. SPONSOR/MONITOR'S ACRONYM(S)			
						11. SPONSOR/MONITOR'S REPORT NUMBER(S)			
12. DISTRIBUTION / AVAILABILITY STATEMENT Approved for public release; distribution unlimited									
13. SUPPLEMENTARY NOTES									
14. ABSTRACT The PCRP Prostate Cancer Training Award has supported my training for the past 12 months. During this time, I have worked towards attaining a better understanding of (a) the biology of prostate cancer, (b) the biology of specific growth factor signaling pathways, (c) the principle and application of cutting edge techniques in modern molecular and cellular biology, and (d) the principle and application of genetically engineered mouse (GEM) models, with the intent of becoming uniquely positioned to investigate the role of specific factor signaling in the initiation, progression and metastasis of spontaneous autochthonous prostate cancer and the emergence of the castration resistant phenotype. In addition to this rigorous technical training, I have continued to attend weekly lab meetings, division wide Cancer Biology Seminar series, and the Pacific Northwest SPORE in Prostate Cancer meetings.									
15. SUBJECT TERMS mouse models, prostate cancer, epithelial cells, transformation									
16. SECURITY CLASSIFICATION OF:						17. LIMITATION OF ABSTRACT UU	18. NUMBER OF PAGES 18	19a. NAME OF RESPONSIBLE PERSON USAMRMC	
a. REPORT U	b. ABSTRACT U	c. THIS PAGE U	19b. TELEPHONE NUMBER (include area code)						

Table of Contents

	<u>Page</u>
Cover	1
Standard Form 298	2
Table of Contents	3
Introduction	4
Body	4
Key Research Accomplishments	8
Reportable Outcomes	9
Conclusions	9
References	9
List of Personnel	10
Appendices	10
Supporting Data	12

Introduction:

After skin cancer, prostate cancer is the leading diagnosed cancer and has the highest mortality in American males (1). It is an increasing health problem in the US and results in many misdiagnoses and unnecessary surgeries. This is due to the fact that there are few predictors of malignancy and that the current standard of care is not specific to the various forms of this disease. The underlying cause for prostate cancer is unknown. However current research is examining several molecular pathways, that have been linked to initiation, progression and development. One such pathway is the Wnt signaling pathway. The Wnt family of proteins are known regulators of embryonic development but have also been implicated in molecular signaling epithelial to mesenchyme transition (EMT) and cancer development (2-7). High levels of Wnt expression have been observed in several cancers including prostate (8). As a consequence, transcription factors downstream in the pathway such as Beta-catenin can be more active. Beta-catenin acts as within the nucleus, regulating several genes thought to be involved in prostate cancer (9). In addition Beta-catenin also acts in conjunction with E-cadherin as a structural component in cellular adhesion. Cellular adhesion is not only important in maintaining cell structural integrity but also in cellular communication and mobility. Adhesion complexes are now recognized as vital players in cell signaling (10). Therefore regulators of cell adhesion including Beta-catenin and E-cadherin are likely directly involved in cancer progression. E-cadherin expression is decreased in several cancers. There are several known regulators of E-cadherin such as Snai1 and Zeb1 (11-13). As with members of the Wnt family, these factors also control elements of embryonic development including the epithelial to mesenchyme transition. This study intended to demonstrate that with enforced expression of Wnt would lead to prostate cancer progression.

The PCRP Prostate Cancer Training Award has continued to support my training. I have worked towards attaining a better understanding of (a) the biology of prostate cancer, (b) the biology of specific growth factor signaling pathways, (c) the principle and application of cutting edge techniques in modern molecular and cellular biology, and (d) the principle and application of genetically engineered mouse (GEM) models, with the intent of becoming uniquely positioned to investigate the role of specific factor signaling in the initiation, progression and metastasis of spontaneous autochthonous prostate cancer and the emergence of the castration resistant phenotype. In addition to this rigorous technical training, I have continued to attend weekly lab meetings, division wide Cancer Biology Seminar series, and the Pacific Northwest SPORE in Prostate Cancer meetings.

Body:

Specific aim 1: Determine the influence of enforced expression of the proto-oncogene, *Wnt3*, on epithelial cells of the mouse prostate.

After I established a quantitative Real-Time PCR (QPCR) based methodology to measure levels of mRNA transcripts encoding E-cadherin, N-cadherin, Cytokeratin-5, Cytokeratin-8, Cytokeratin-14, Cytokeratin-18, Cytokeratin-19, Synaptophysin, Chromogranin A, Slug, Snai1, Smooth Muscle Actin, Vimentin, Androgen Receptor, Insulin like Growth Factor-1, Ki-67 and Zeb1 and 2. All the E-box transcription factors except Zeb2 showed an increase in mRNA levels with Slug having almost 20% more expression compared to control (Figure 1B). We also noted decreased expression Cyclin D1 and Cytokeratin 5 in the Wnt3-IRES-Luc mice compared to controls. Notably, we became interested in how mis-regulation of the Snail E-box repressor during transformation facilitates the epithelial-mesenchymal transition and we decided to

exploit a line of “floxed” Snai1 mice to test the hypothesis that deregulated Snai1 expression facilitates a more aggressive metastatic disease.

The complete knockdown of Snai1, results in embryonic lethality at embryonic day 9.5. Therefore we created a conditional knockdown of Snai1 expression in C57/BL6 background, mouse prostates. Using a floxed Snai1 gene (Snai1^{f/f}) mouse provided by Thomas Gridley at the Jackson labs, we crossed this to mice expressing Cre- recombinase under the prostate specific probasin promoter (PBCRE). We then crossed the homozygous Snai1^{f/f} mice with the TRansgenic Adenocarcinoma of the Mouse Prostate (TRAMP) mouse to examine prostate tumor formation. The TRAMP mouse resembles human prostate cancer pathology, whereby male mice develop spontaneous orthotopic prostate tumors following puberty (12 weeks). The progeny of these crosses were then genotyped for Snai1^{f/f} homozygosity, PBCRE and TRAMP (Figure 2). Briefly the dorsal/lateral prostate lobes were dissected and total RNA from the lobes was extracted using the RNeasy kit from Qiagen (Valencia, CA) according to the manufacturer’s protocol. Total RNA was reverse transcribed using SuperScriptII reverse transcriptase and an oligo dT primer from Invitrogen (Carlsbad, CA). Standard PCR was conducted using primers for floxed Snai1, deleted Snai1, PBCRE, TRAMP and Actin (Table 2).

We then examined the histopathologic changes in the prostate lobes and any tumors from these mice (Figure 3). Thirty-week old mouse prostate lobes and any tumors were dissected from Snai1^{f/f} x PBCRE positive/negative and TRAMP positive/negative. These lobes were 10% formalin for 24 hours and then 70% ethanol fixed for 48 hours. Fixed sections were paraffin embedded and cut into 8 um sections which were subjected to hemotoxylin/eosin or trichrome staining. All prostate lobes: anterior, dorsal, lateral and ventral were examined for gross changes in morphology. Snai1^{f/f} mice, positive or negative for PBCRE and negative for TRAMP appeared normal. This indicated to us that the absence of Snai1 by itself had no effect on normal prostate morphology. Similarly Snai1^{f/f} mice that were negative for PBCRE but positive for TRAMP displayed the expected phenotype. The anterior, dorsal and ventral lobes showed increased cell numbers with cells entering adjacent lumens. In contrast, Snai1^{f/f} mice positive for both PBCRE and TRAMP positive, clearly showed infiltration of luminal cells into adjacent lumens and a more discontinuous morphology compared to PBCRE negative TRAMP positive lobes although they did not show a net increase in cell numbers. The phenotype observed as a consequence of loss of Snai1 appears to be indicative of a change in cell adhesion. This change in cell adhesion was unexpected as decreased Snai1, a negative regulator of the adhesion protein E-cadherin, would be expected to increase E-cadherin and stabilize adhesion. The loss of adhesion indicates that Snai1 may also act to maintain prostate cell adhesion and prostate lobe integrity.

To further examine the role of Snai1 in prostate tumor formation we further interrogated the Snai1^{f/f} x PBCRE x TRAMP mice by immunohistochemical analysis of E-cadherin, Beta-catenin, Snai1 and Zeb1 (Figure 4). Some Snai1 expression was seen in prostate lobes except in PBCRE positive mice. Since Snai1 is a known regulator of E-cadherin expression, we saw little change in E-cadherin expression in tissues lacking Snai1 expression, compared to those with normal expression (Figures 3, and 4). As expected, E-cadherin was maintained in the epithelial layer of all prostate lobes. Zeb1 expression was seen mostly localized to the stroma (data not shown). However we did see changes in Beta-catenin expression. Prostate tissue sections from TRAMP mice with Snai1 knockdown showed that Beta-catenin protein expression was reduced to undetectable levels in several prostate luminal epithelial cells. When comparing TRAMP positive mouse prostates harboring normal Snai1 we noted that Beta-catenin expression was maintained. Interestingly, Beta-catenin localization normally mimics the E-cadherin pattern but this was greatly disrupted in Snai1^{f/f} mice that were PBCRE positive and TRAMP positive. Therefore the change in prostate cell adhesion was likely due to Snai1 directly or indirectly stabilizing Beta-catenin protein at the cell membrane. We did not note any significant change in Beta-catenin translocation to the nucleus. Therefore it appears that Snai1 may also regulate Beta-catenin expression. This regulation could be indirect because there are no apparent E-box regulatory regions on the proximal Beta-catenin promoter.

To further examine the expression of Beta-catenin, E-cadherin, Snai1, and Zeb1, we used real-time PCR. We also analyzed expression of EMT associated genes Calponin and Vimentin, both mesenchymal markers in Snailf/f/ x PBCRE x TRAMP mice (Figure 5). We normalized expression to ribosomal protein S16 and made expression relative to Snailf/f/ x PBCRE negative/TRAMP negative samples. Snailf/f/ mice that were PBCRE negative but TRAMP positive showed increased levels of E-cadherin, Snai1 and Zeb1. These mice also had decreased levels of Beta-catenin, Calponin and Vimentin. Whole prostates from Snailf/f/ mice positive for PBCRE and either negative or positive for TRAMP showed decreased expression in Snai1, E-cadherin, Calponin, Vimentin and no change in Zeb1 expression. However we noted an increase in Beta-catenin expression. This indicates that while disruption of Beta-catenin membrane localization occurs in the absence of Snai1, the expression level increases. The lower levels of E-cadherin could be due to a possible feedback mechanism with Snai1 or compensatory mechanisms from other EMT regulators.

We also examined Snai1 in cultured mouse prostate cells. C2H cells are mouse prostate cells derived from TRAMP mouse prostates. These cells were grown on glass cover slips in six-well cultured plates for 48 hours. After media was removed cells were then fixed in 4% formaldehyde/phosphate buffer solution for 20 minutes at room temperature. Cover slips were permeabilized using a 0.1% TritonX-100/phosphate buffered solution for 2 minutes at room temperature. Coverslips were blocked in a 5% BSA/phosphate buffered solution at room temperature for 2 hours. Each coverslip was then exposed to a primary antibody for 1 hour at room temperature. Next coverslips were washed three times for 5 minutes with phosphate buffered solution (PBS). Next, coverslips were exposed to a fluorescent secondary antibody (Alexa-Fluor 594, Invitrogen, Carlsbad, CA) for 1 hour at room temperature. Coverslips were washed three times for 5 minutes with PBS and mounted with fluoromount with DAPI (Vector Labs, Burlingame, CA) on glass slides. Photos were taken using a Nikon fluorescent microscope with the 40 or 60X oil objective. Cell nuclei were visualized by observation of DAPI staining through the 400 nm “blue” channel filter. Staining of Snai1 or Zeb1 was through observation through the 594 nm “red” channel filter. Images were taken utilizing MagnaFire v2.0 (Karl Storz Imaging, Germany) software on a Mac operating system.

C2H cells grown in culture on coverslips showed specific nuclear Zeb1 localization but no detectable Snai1 (Figure 6). However we noted both Zeb1 and Snai1 are expressed by C2H when these cells were grafted into NOD/SCID mice (Figure 7). In these studies approximately 10,000 cells were injected into the flanks of NOD/SCID mice and allowed to grow for 30 days. Growths were excised and analyzed as above. While Zeb1 expression in C2H cells was present in both cultured and tumor sections, Snai1 expression was seen only in the grafted tumors. This reflects a role of Snai1 in tumor progression in the in vivo mouse model. Interestingly, when we examined C2H mRNA expression through real time analysis we noted that Zeb1 and Snai1 were equally expressed. Therefore Snai1 protein is not active in cultured cells but appears up regulated in C2H tumors. The mechanism of Snai1 regulation in C2H mouse prostate cells is not known but is being investigated.

Further analysis of conditional knock out (cKO) Snai1 mice indicates that there is a change in growth of cells in the prostate (Figure 8). As expected, E-cadherin expression was maintained with the prostate specific loss of Snai1. However Beta-catenin localization was unusual in Snai1 cKO mice when compared to control mice. After observing abnormalities in the prostates in the Snai1 cKO mice we next wanted to test the consequence of titrating Snai1 expression in cultured mouse prostate cell lines (Figure 6). We choose C2H cells that are derived from TRAMP mouse prostate cells. As discussed C2H cells do not express high levels of Snai1 in culture but do so as mouse grafts. We decreased Snai1 and Zeb1 expression in C2H cells by shRNA and treated them with 10 nM R1881 a testosterone analog or vehicle in serum free media. After seeding cells in six well plates we observed the growth rates after 2 days owing to the transitory nature of the shRNA. Cells transfected with shRNA and treated with R1881 showed a decrease in cell numbers after one day, but quickly recovered. Cells treated with a non-specific scramble shRNA showed a slight increase in growth when treated with R1881. We noted that cells transfected with shRNA for GAPDH had a decreased growth rate but returned to normal when treated with R1881 as compared to the scrambled control. In contrast C2H cells transfected with shRNA for Snai1 showed a reduced rate of growth but did not change rates when treated with R1881. And

cells transfected with shRNA for Zeb1 showed a high level of growth but severely reduced growth when treated with R1881. When correlated with protein and RNA expression levels we see that while the knockdown of Snai1 has little effect on C2H growth rate the loss of Zeb1 and addition of testosterone (R1881) can decrease cell growth. This indicates that C2H mouse prostate cells lines are dependent on Zeb1 for growth and that testosterone limits this growth indicating the antagonism between androgen receptor and Zeb1 activity.

We also noted that there was increased cellular proliferation in TRAMP positive mice with normal Snai1 expression when compared to Snai1f/f/ x PBCRE x TRAMP positive mice (Figure 8). Even though proliferation was decreased in Snai1f/f/ x PBCRE x TRAMP positive mice, luminal epithelial cells showed a loss of adhesion, resulting in grossly abnormal prostate lobes when compared to TRAMP positive mice with normal Snai1 expression. TRAMP positive mice with normal Snai1 expression formed localized nodes of epithelial cellular proliferation that maintained prostate lobe architecture and consistent division between luminal and stroma cell layers. In contrast the Snai1f/f x PBCRE x TRAMP positive mice had indistinguishable luminal and stromal layers. Cells appeared detached, and occupied their respective lumens. This phenomenon of loose luminal epithelial cells was only observed with Snai1f/f/ x PBCRE x TRAMP positive mice. Mice with Snai1f/f/ x PBCRE but TRAMP negative did not show this phenotype and had prostate lobes that resembled normal wild-type (TRAMP negative) control prostates. The effect of TRAMP, a driver of the SV40 large T and little t antigen in mouse prostates is to induce tumor formation. Tumor formation is the result of the viral oncoprotein regulating other oncogenes. Therefore the loss of Snai1 while maintaining E-cadherin expression in TRAMP positive mouse prostate tumors alters Beta-catenin protein expression. Beta-catenin protein turnover is regulated by GSK-3 phosphorylation. GSK-3 is in turn regulated by Wnt signaling. Active Wnt signaling down regulates GSK-3, thus stabilizes Beta-catenin. Beta-catenin then acts a transcription factor and translocates to the nucleus. But this is not seen in the Snai1 knockdown mice. Perhaps the maintained expression of E-cadherin and its association with Beta-catenin dissuades nuclear translocation and is blocked from preventing eventual Beta-catenin destruction. So abnormal Beta-catenin turnover occurs in the absence of Snai1. We also examined expression of Beta catenin in TRAMP mice through real-time PCR analysis. The expression of Beta-catenin is elevated in Snai1 cKO TRAMP positive mice compared to control and TRAMP positive mice with intact Snai1. Therefore the loss of the transcription factor regulator Snai1, results in the up regulation of Beta-catenin. Snai1 acts to repress E-cadherin by binding to E-box regulatory regions within the E-cadherin gene promoter. There are no proximal E-box regulatory regions known within the Beta-catenin promoter. Therefore there does not appear to be any direct regulatory relationship between Snai1 and Beta-catenin. We can then surmise that Beta-catenin while up regulated in TRAMP positive mouse prostates is also indirectly regulated by Snai1. The mechanism of this regulation is not yet understood but may involve the Wnt pathway.

Specific aim 2: Determine the influence of enforced Wnt3 expression during tumor progression and metastasis in the transgenic adenocarcinoma of the mouse prostate (TRAMP) model.

(Non specific expression seen in our transgenic Wnt3 mice. We are now trying to subclone into ROSA26 locus).

We are still waiting to select the lines with the highest spatially restricted expression of *Wnt* prior to crossing to TRAMP.

Specific aim 3: Develop lines of reporter mice to detect activation of the Wnt/Beta-catenin pathway *in vivo* during normal development and cancer progression.

These studies are ongoing and we are refining our imaging technology.

Methods:

Cells

Cultured cells were kept in a humidified 5% CO₂ 42C incubator. C2H cells were maintained in Dulbecco's Modified Eagle Media (DMEM) with 10% fetal bovine serum, 1% penicillin/streptomycin antibiotic.

Mice

Strains and breeding. All animal studies were conducted in accordance with institutional guidelines for humane animal treatment. Mice were maintained at 22°C in a 12-h light and dark cycle with ad libitum access to water and food. Mice homozygous for the Wnt3 IRES-Luc mice transgene were maintained in a pure FVB/NJ background. Mice homozygous for the Snai1f/f/, PBCRE and TRAMP transgenes were maintained in a C57/BL background.

RNA preparation and PCR analysis

Total RNA was extracted from separate lobes of the mouse prostate using the RNAeasy kit (Qiagen, Valencia, CA) following the manufacturer's recommendations. Briefly, mouse prostates were immediately dissected from euthanized mice. The ventral, anterior, dorsal and lateral prostate lobes were separated and placed in RNA later stabilization buffer (Qiagen, Valencia CA). Samples were then homogenized and RNA extracted, purified and resuspended in RNase free water. Purified RNA was then quantitated on NanoDrop UV-Vis spectrophotometer (Thermo Fisher, Waltham, MA). Total RNA (1 µg) was reverse transcribed using an SuperScript II First-Strand synthesis kit. (Invitrogen, Carlsbad, CA). Briefly, following manufacturer's instructions RNA was denatured at 72°C for 10 mins then 200 U for MMLV reverse transcriptase enzyme were used along with oligo dT primers in a final reaction of 20 µl. Freshly reverse transcribed cDNA (1 µl) was used for real-time RT-PCR with mouse-specific primers for genes as shown in Table 1. DNA synthesis was monitored via the fluorescent dye SYBR Green present in HotStart-IT SYBR Green qPCR Master Mix, (USB Corporation, Cleveland OH), using the Bio-Rad real-time DNA amplification system (Bio-Rad, Hercules, CA). The following protocol was used; a 95°C denaturation step for 5 min followed by 40 cycles with denaturation for 1 min at 95°C, annealing for 1 min at 58 C, and extension for 1 min sec at 72°C. Gene expression was normalized to mouse ribosomal protein gene S16 or mouse Beta-actin. PCR products were subjected to a melting curve analysis, and the data were analyzed and quantified with the MyiQ analysis software (Bio-Rad, Hercules CA). The relative quantitative value for each target gene compared with the calibrator for the target was expressed as comparative Ct ($2^{-\Delta Ct-Cc}$) method (Ct and Cc are the mean threshold cycle differences after normalizing to 16 S). Real-time RT-PCR experiments were performed in triplicate and the percent coefficient of variation for the set value was less than 0.1. PCR efficiency with given primers was between 95 and 105%. Relative percent gene expression level changes in Wnt 3 IRES-Luc positive mice were then compared to negative control littermate gene expression.

C2H shRNA (Ambion, Austin TX) cell count assay

Cells were equally plated into 6 well dishes in 10% FBS DMEM with phenol red media.

The next day cells were counted by trypsin harvesting and using trypan blue to give an approximate number of cells prior to transfection. Cells kept in wells were transfected using the Ambion siPORT amine transfection reagent and utilizing the manufacturer's recommended protocol for transfections for adherent cells in a standard 6-well plate. Briefly 6 µl of siPORT Amine transfection reagent was diluted into 100 µl of OPTI-MEM low serum media and incubated at room temperature for 10 minutes. The pre-designed siRNA oligos were obtained from the Silencer Select catalogue from Ambion. Approximately 2 µl of either Snai1, Zeb1, GAPDH or Scrambled siRNA was used per well. To create the transfection formulations, OPTI-MEM was added to a total volume of 2.5 mL replaced over standard 10% FBS DMEM growth media for 24 hours. Media was replaced after the 24 hour transfection period with 10% FBS DMEM growth media. Cells were harvested and counted 24 and 48 hours after transfection using trypan blue staining.

Key Research Accomplishments:

- Created novel real time quantitative PCR based method to measure specific mRNA transcripts related to epithelial differentiation and detect epithelial to mesenchymal transitions.
- Created transgenic mouse model with prostate specific knock-down of Snai1.
- Created immunofluorescent method to examine EMT markers in mouse prostate tissue sections.
- Established growth assay to examine cell lines with knock-down of Snai1 or Zeb1

Reportable Outcomes:

- Quantitative analysis of Wnt3 prostate mRNA.
- Quantitative analysis of EMT markers (Snai1 and Zeb1) from mouse prostate cells.
- Over expression of Wnt3 in mouse prostates causes an upregulation in Snai1 and Zeb1 expression.
- Levels of Snai1 mRNA and protein expression are decreased in Snai1f/f/ x PBCRE x TRAMP mice.
- Levels of E-cadherin mRNA are decreased but protein expression is maintained in Snai1f/f/ x PBCRE x TRAMP positive mice.
- The deletion of Snai1 also causes an increase in Beta-catenin gene expression but a decrease in membrane Beta catenin localization Snai1f/f/ x PBCRE x TRAMP positive mice.
- The deletion of Snai1 from TRAMP positive mouse prostate epithelial cells results in disruption of cell adhesion.
- The shRNA knock down of Snai1 and Zeb1 in cultured mouse prostate cells also results in decreased growth rate.

Conclusions:

The results of this work support that growth factor signaling pathways such as Wnt are related to tumorigenesis in the mouse prostate. Hence, Wnt signaling promotes prostate cancer in the mouse. Furthermore, we feel that cooperation between the Wnt and E-box repressor Snail will facilitate more aggressive metastatic disease and may actually increase the frequency or size of osteoblastic bone metastases. Our current QPCR data suggests that Wnt3 may have a role in regulating Snai1 and other genes related to cell morphology. It appears that Snai1 is an important component in mouse prostate tumor progression and involved with cellular adhesion. Snai1 appears to regulate not only E-cadherin expression but also Beta-catenin expression as well. We noted that the loss of Snai1 resulted in a slight decrease of E-cadherin expression and an increase in Beta-catenin. There was no change in E-cadherin localization but there was an apparent change in Beta-catenin localization in mouse TRAMP prostates. Other EMT markers such as Zeb1 and Slug also may play a role in TRAMP mouse prostate cancer progression and may serve to compensate for the lack of Snai1 in our knock-out mice. Therefore if Wnt signaling may be involved with regulation of both Beta-catenin and Snai1. This level of control culminates in the regulation of cell adhesion and proliferation in prostate tumor progression.

References:

1. Horner MJ, Ries LAG, Krapcho M, Neyman N, Aminou R, Howlader N, Altekruse SF, Feuer EJ, Huang L, Mariotto A, Miller BA, Lewis DR, Eisner MP, Stinchcomb DG, Edwards BK (eds). *SEER Cancer Statistics Review, 1975-2006*, National Cancer Institute. Bethesda, MD
2. Katoh M, Katoh M., *Cancer Biol Ther.* 2006 Sep;5(9):1059-64.
3. Yook JI, Li XY, Ota I, Hu C, Kim HS, Kim NH, Cha SY, Ryu JK, Choi YJ, Kim J, Fearon ER, Weiss SJ. *Nat Cell Biol.* 2006 Dec;8(12):1398-406.
4. Moustakas A, Heldin CH., *Cancer Sci.* 2007 Oct;98(10):1512-20.
5. Tommasi S, Pinto R, Pilato B, Paradiso A., *Curr Pharm Des.* 2007;13(32):3279-87.
6. Stemmer V, de Craene B, Berx G, Behrens J., *Oncogene.* 2008 Aug 28;27(37):5075-80.
7. Taki M, Kamata N, Yokoyama K, Fujimoto R, Tsutsumi S, Nagayama M., *Cancer Sci.* 2003 Jul;94(7):593-7.

8. Vincent T, Neve EP, Johnson JR, Kukalev A, Rojo F, Albanell J, Pietras K, Virtanen I, Philipson L, Leopold PL, Crystal RG, de Herreros AG, Moustakas A, Pettersson RF, Fuxe J., *Nat Cell Biol.* 2009 Aug;11(8):943-50.
9. Laux H, Tomer R, Mader MT, Smida J, Budczies J, Kappler R, Hahn H, Blöching M, Schnitzbauer U, Eckardt-Schupp F, Höfler H, Becker KF., *Lab Invest.* 2004 Oct;84(10):1372-86.
10. de Yzaguirre MM, Hernández JS, Navarro PF, Nieva PL, Herranz M, Fraga MF, Esteller M, Juarranz A, Fernández-Piqueras J., *Carcinogenesis.* 2006 May;27(5):1081-9.
11. Drake JM, Strohbahn G, Bair TB, Moreland JG, Henry MD., *Mol Biol Cell.* 2009 Apr;20(8):2207-17.
12. Graham TR, Yacoub R, Taliaferro-Smith L, Osunkoya AO, Odeero-Marah VA, Liu T, Kimbro KS, Sharma D, O'Regan RM., *Breast Cancer Res Treat.* 2009 Nov 18
13. Schmalhofer O, Brabletz S, Brabletz T., *Cancer Metastasis Rev.* 2009 Jun;28(1-2):151-66.

List of Personnel:

Robin Tharakan (Principal Investigator)

Appendices:

Progress Report

January 1, 2009.

PCRP Prostate Cancer Training Award #W81XWH-07-1-0039

PI: Robin Tharakan, Ph.D.

Introduction:

The PCRP Prostate Cancer Training Award has supported my training for the past 12 months. During this time, I have worked towards attaining a better understanding of (a) the biology of prostate cancer, (b) the biology of specific growth factor signaling pathways, (c) the principle and application of cutting edge techniques in modern molecular and cellular biology, and (d) the principle and application of genetically engineered mouse (GEM) models, with the intent of becoming uniquely positioned to investigate the role of specific factor signaling in the initiation, progression and metastasis of spontaneous autochthonous prostate cancer and the emergence of the castration resistant phenotype. In addition to this rigorous technical training, I have continued to attend weekly lab meetings, division wide Cancer Biology Seminar series, and the Pacific Northwest SPORE in Prostate Cancer meetings.

Body:

Specific aim 1: Determine the influence of enforced expression of the proto-oncogene, *Wnt3*, on epithelial cells of the mouse prostate.

After I assumed responsibility for this project I immediately immersed myself in studying the biology of the epithelial and stromal compartments of the mouse prostate. To this end I decided to create assays that would allow me to measure quantitatively changes in expression of various markers that were intricately associated with epithelial and stromal differentiation. This was deemed necessary to elucidate the phenotypic consequence of deregulated growth factor expression in the transgenic models as previously described by Dr. Houghtaling. Of note, I established a quantitative RT-PCR (QPCR) based methodology to measure levels of mRNA transcripts encoding E-cadherin, N-cadherin, Cytokeratin-5, Cytokeratin-8, Cytokeratin-14, Cytokeratin-18, Cytokeratin-19, Synaptophysin, Chromogranin A, Slug, Snail, Smooth Muscle Actin, Vimentin, Androgen receptor, Insulin like Growth Factor-1, Ki-67 and Zebs 1 and 2. I am currently expanding the assay to include

various specific targets in the Wnt/TCF signaling pathway. As the mice previously generated by Dr. Houghtaling become older I will perform detailed analysis of the histology and use the RT-PCR methods to measure specific changes in gene expression as a function of time. QPCR analysis on Wnt3 IRES-Luc mice are presented in Figures 1A and 1B. I noted changes in the mRNA levels of several genes of Wnt3 IRES-Luc positive mice compared to non transgenic littermates. The Wnt3 transgenic mouse had over 40% increase in mRNA levels compared to non transgenic littermate controls (Figure 1A). This is not unexpected as this mouse was engineered to over express the Wnt3 gene. Cytokeratin 18 was the only tested cytokeratin with a marked 42% increase in mRNA levels compared to littermate controls (Figure 1A). Both Vimentin and Calponin also showed increased expression, 19% and 25 % respectively in Wnt3 IRES-Luc mice compared to non transgenic controls (Figure 1A). All the E-box transcription factors except Zeb2 showed an increase in mRNA levels with Slug having almost 20% more expression compared to control (Figure 1B). We also noted decreased expression cyclin D1 and cytokeratin 5 in the Wnt3-IRES-Luc mice compared to controls. We continue to test the hypothesis that inappropriate expression of *Wnt3* and other members of the Wnt family (specifically *Wnt4*) will be able to cause the transformation of the mouse prostate. Notably, we are also interested in how misregulation of the Snail E-box repressor during transformation facilitates the epithelial-mesenchymal transition and we hope to eventually cross a line of Snail^{LoxP} mice with the mice misexpressing *Wnt3* (or *Wnt4*) to test the hypothesis that deregulated Slug or Snail expression facilitates a more aggressive metastatic disease.

Specific aim 2: Determine the influence of enforced Wnt3 expression during tumor progression and metastasis in the transgenic adenocarcinoma of the mouse prostate (TRAMP) model.

We are still waiting to select the lines with the highest spatially restricted expression of *Wnt* prior to crossing to TRAMP.

Specific aim 3: Develop lines of reporter mice to detect activation of the Wnt/ β -catenin pathway *in vivo* during normal development and cancer progression.

These studies are ongoing and we are refining our imaging technology.

Methods:

Mice

Strains and breeding. All animal studies were conducted in accordance with institutional guidelines for humane animal treatment. Mice were maintained at 22°C in a 12-h light and dark cycle with ad libitum access to water and food. Mice homozygous for the Wnt3 IRES-Luc mice transgene were maintained in a pure FVB/NJ background.

RNA preparation and PCR analysis

Total RNA was extracted from separate lobes of the mouse prostate using the RNeasy kit (Qiagen, Valencia, CA) following the manufacturer's recommendations. Briefly, mouse prostates were immediately dissected from euthanized mice. The ventral, anterior, dorsal and lateral prostate lobes were separated and placed in RNA later stabilization buffer (Qiagen, Valencia, CA). Samples were then homogenized and RNA extracted, purified and resuspended in RNase free water. Purified RNA was then quantitated on NanoDrop UV-Vis spectrophotometer (Thermo Fisher, Waltham, MA). Total RNA (1 μ g) was reverse transcribed using an SuperScript II First-Strand synthesis kit. (Invitrogen, Carlsbad, CA). Briefly, following manufacturer's instructions RNA was denatured at 72°C for 10 mins then 200 U for MMLV reverse transcriptase enzyme were used along with oligo dT primers in a final reaction of 20 μ l. Freshly reverse transcribed cDNA (1 μ l) was used for real-time RT-PCR with mouse-specific primers for genes as shown in Table 1. DNA synthesis was monitored via the fluorescent dye SYBR Green present in HotStart-IT SYBR Green qPCR Master Mix, (USB Corporation, Cleveland OH), using the Bio-Rad real-time DNA amplification system (Bio-Rad, Hercules, CA). The following protocol was used; a 95°C denaturation step for 5 min followed by 40 cycles with denaturation for 1 min at 95°C, annealing for 1 min at 58 C, and extension for 1 min sec at 72°C. Gene expression was normalized to mouse ribosomal protein gene S16 or mouse Beta-actin. PCR products were subjected to a melting curve analysis, and the data were analyzed

and quantified with the MyiQ analysis software (Bio-Rad, Hercules, CA). The relative quantitative value for each target gene compared with the calibrator for the target was expressed as comparative Ct ($2^{-\Delta C_t-C_c}$) method (Ct and Cc are the mean threshold cycle differences after normalizing to 16 S). Real-time RT-PCR experiments were performed in triplicate and the percent coefficient of variation for the set value was less than 0.1. PCR efficiency with given primers was between 95 and 105%. Relative percent gene expression level changes in Wnt 3 IRES-Luc positive mice were then compared to negative control littermate gene expression.

Key Research Accomplishments: Created novel real time quantitative PCR based method to measure specific mRNA transcripts related to epithelial differentiation and detect epithelial to mesenchymal transitions.

Reportable Outcomes: Quantitative analysis of Wnt3 prostate mRNA.

Conclusions:

The results of this work should support or refute the hypothesis that enforced expression of growth factor signaling pathways such as Wnt is sufficient to drive tumorigenesis in the mouse prostate. We are now prepared to measure the quantitative increase in the GU weight to support the central hypothesis that deregulated Wnt signaling promotes prostate cancer in the mouse. Furthermore, we feel that cooperation between the *Wnt* and E-box repressors like Slug and Snail will facilitate more aggressive metastatic disease and increase the frequency or size of osteoblastic bone metastases. Our current QPCR data suggests that Wnt3 may have a role in regulating Slug and other genes related to cell morphology. Our future studies with the Wnt3 mice bred with our TRAMP mice may reveal the role of Wnt3 regulation in prostate cancer progression.

References: none

Appendices: none

Supporting Data:

Table 1. Real Time PCR Primer Sets

Gene	Primer Sequence
Androgen Receptor	Forward 5' AACAGCAGCAGGAGGTAATCTCCGA 3' Reverse 5' GGC GTAACCTCCCTTGAAAGAGGAA 3'
Axin 2	Forward 5' CTCCTTGGAGGCAAGAGC Reverse 5' GGCCACGCAGCACCGCTG
Beta-Actin	Forward 5' GTGGGCCCGCCCTAGGCACCAA Reverse 5' CTCTTTGATGTCACGCACGATTTC
Calponin	Forward 5' GCACATTTTAACCGAGGTCC Reverse 5' TGACCTTCTTCACAGAACCC
Chromogranin A	Forward 5' CAGCAGCTTTGAGGATGAACT Reverse 5' CTGGTTAGGCTCTGGAAAGG
c-Myc	Forward 5' TCTCCACTCACCAGCACAACACTACG Reverse 5' ATCTGCTTCAGGACCCT

Cyclin D1	Forward 5' CTGGCCATGAACTACCTGGA Reverse 5' ATCCGCCTCTGGCATTTTGG
Cytokeratin 5	Forward 5' TCAAGAAGCAGTGTGCCAAC Reverse 5' TCCAGCAGCTTCCTGTTAGGT
Cytokeratin 8	Forward 5' ACATCAACAACCTCCGCCG Reverse 5' TCCATAGACAGCACCACAGACG
Cytokeratin14	Forward 5' AAGGGCTCTTGTGGTATCGGTG Reverse 5' CCAAACTGCTGCTGCTGAAG
Cytokeratin 18	Forward 5' ATGCCCCAAATCTCAGGAC Reverse 5' CCAAGTCAATCTCCAAGGTCTGG
Cytokeratin 19	Forward 5' TTCAGTACGCATTGGGTCAG Reverse 5' GCCAGGGTCCCCTAAAAC
E-cadherin	Forward 5' GACAACGCTCCTGTCTTCAAC Reverse 5' TCTGTGACAACAACGAACTGC
IGF I	Forward 5' TCGTCTTCACACCTCTTCTACCTGG Reverse 5' TGCTTTTGTAGGCTTCAGTGGGGCA
IRS I	Forward 5' AAGCCCAAGAGTATGCATAAGCGCT Reverse 5' AGCGTCTGATATTCATCAGCTGCAG
Ki67	Forward 5' ACAGGCTCCGTA CTTTCCAAT Reverse 5' ACCGGAGTCTTCTTCTCAAGG
N-cadherin	Forward 5' ATTGTCTGATCCTGCCAACTG Reverse 5' CAGTGTTCTGTCCCCTCAT
S16	Forward 5' AGGAGCGATTTGCTGGTGTGGA Reverse 5' GCTACCAGGCCTTTGAGATGGA
Slug	Forward 5' AGATCTGTGGCAAGGCTTTCT Reverse 5' GGAGCAGTTTTTGCCTGGTA
Smooth Muscle Actin	Forward 5' CGATAGAACACGGCATCATC Reverse 5' CATCAGGCAGTTCGTAGCTC
Snai1	Forward 5' CAACTATAGCGAGCTGCAGGA Reverse 5' ACTTGGGGTACCAGGAGAGAGT
Synaptophysin	Forward 5' GTGGTTATCAACCCGATTACG Reverse 5' CAGGCCTTCTCTTGAGCTCTT
Vimentin	Forward 5' GTTTCCAAGCCTGACCTCACTG Reverse 5' CTCTTCCATCTCACGCATCTGG

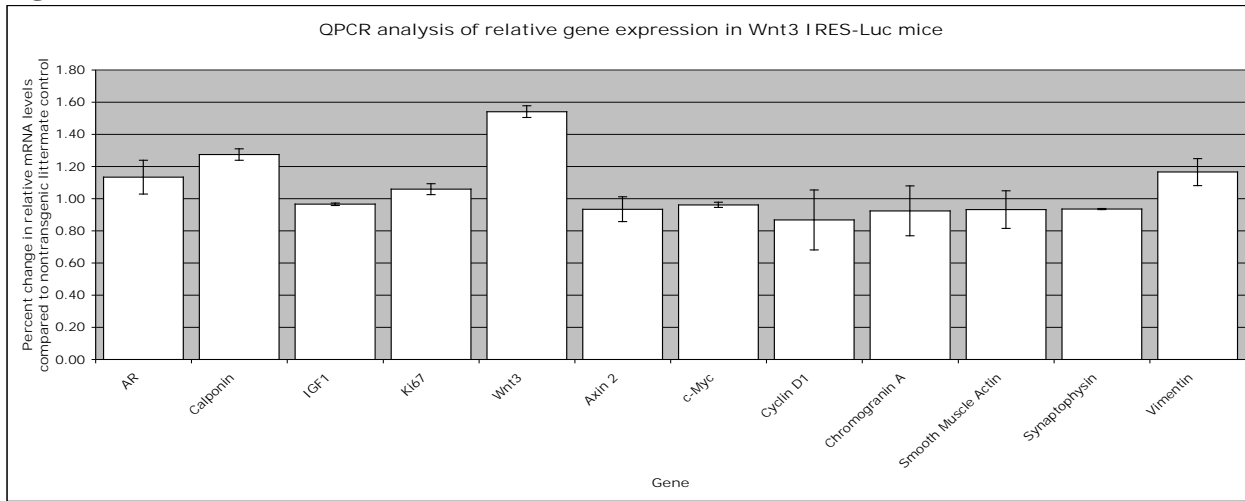
Wnt 3 Forward 5' AAATTGGGTAGCCAGCGAGGAC
Reverse 5' ACTTCAGGGTGAGTTTGGGGAC

VE-cadherin Forward 5' GTTCACCTTCTGTGAGGAGATGG
Reverse 5' ATCTCCAGCGCACTCTTGCTAT

Zeb 1 Forward 5' GGAAACCGCAAGTTCAAGTG
Reverse 5' CACCACACCCTGAGGAGAAC

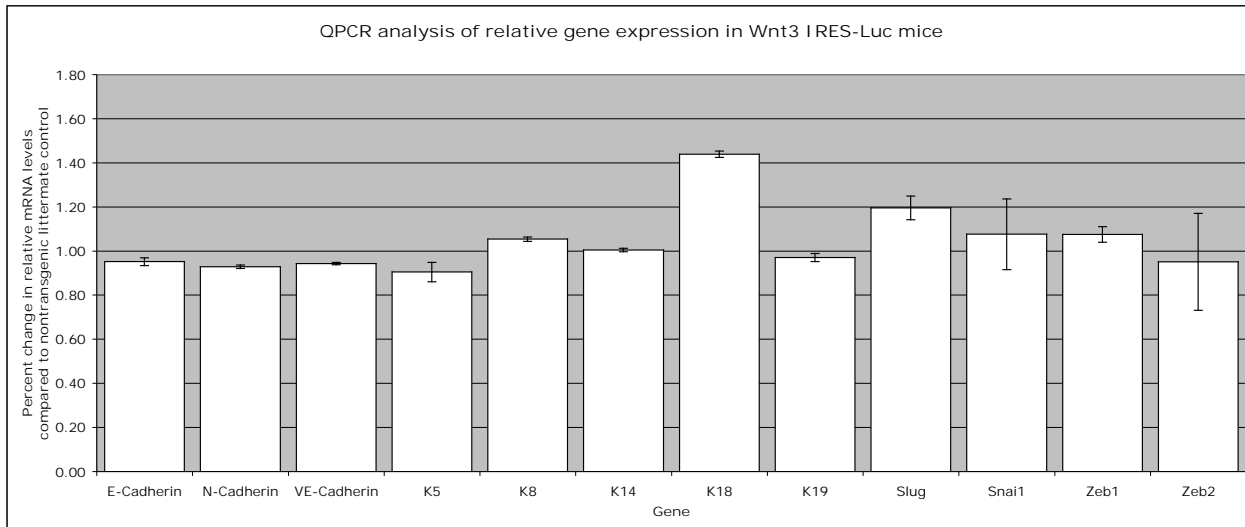
Zeb 2 Forward 5' AGCTCGAGAGGCATATGGTG
Reverse 5' TGTTTCTCATTTCGGCCATTT

Figure 1A.



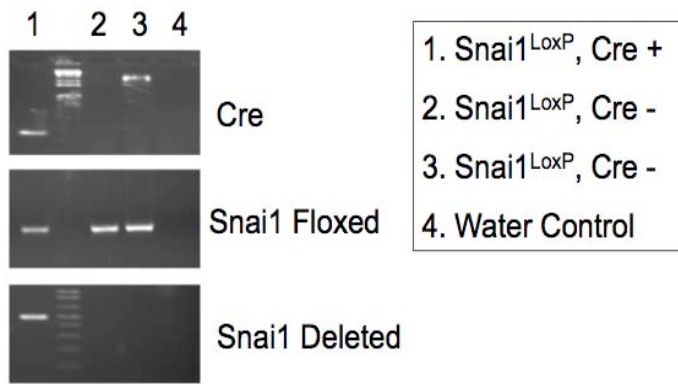
Quantitative real-time PCR analysis detecting mRNA levels of Wnt regulated and other target genes detected in the ventral prostate of 12 week Wnt3 IRES-Luc mice. Samples were done in triplicate and compared to non transgenic littermate mRNA levels that were set to one.

Figure 1B.



Quantitative real-time PCR analysis detecting mRNA levels of cadherin, cytokeratins and E-box transcription factor related genes detected in the ventral prostate of 12 week Wnt3 IRES-Luc mice. Samples were done in triplicate and compared to non transgenic littermate mRNA levels that were set to one.

Figure 2. Standard PCR detection of Snai1 mouse dorsal/lateral prostates.

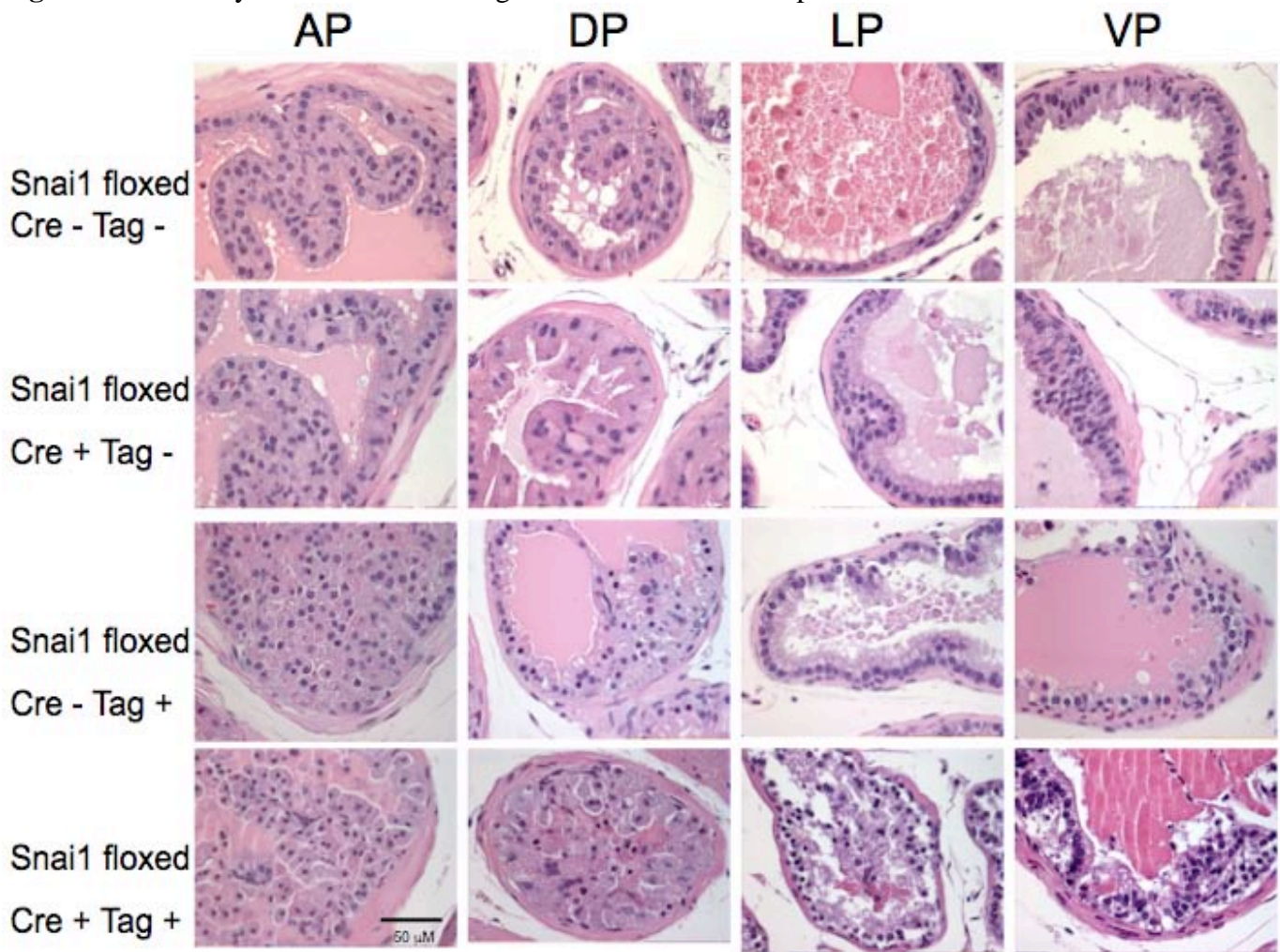


Snai1 deficient mice are embryonic lethal. Therefore we generated mice in which Snai1 is inactivated utilizing Cre/loxP mediated recombination. C57/BL6 Snai1f/f/ mice were crossed with Cre expressing, C57/BL6 TRAMP mice. Snai1 was inactivated specifically in the prostate using a probasin promoter driven Cre recombinase. PCR analysis from mouse prostates indicate the recombination and loss of Snai1 expression in Snai1f/f/ mice expressing PBCRE.

Table 2. Primer sets used for standard and real time PCR analysis:

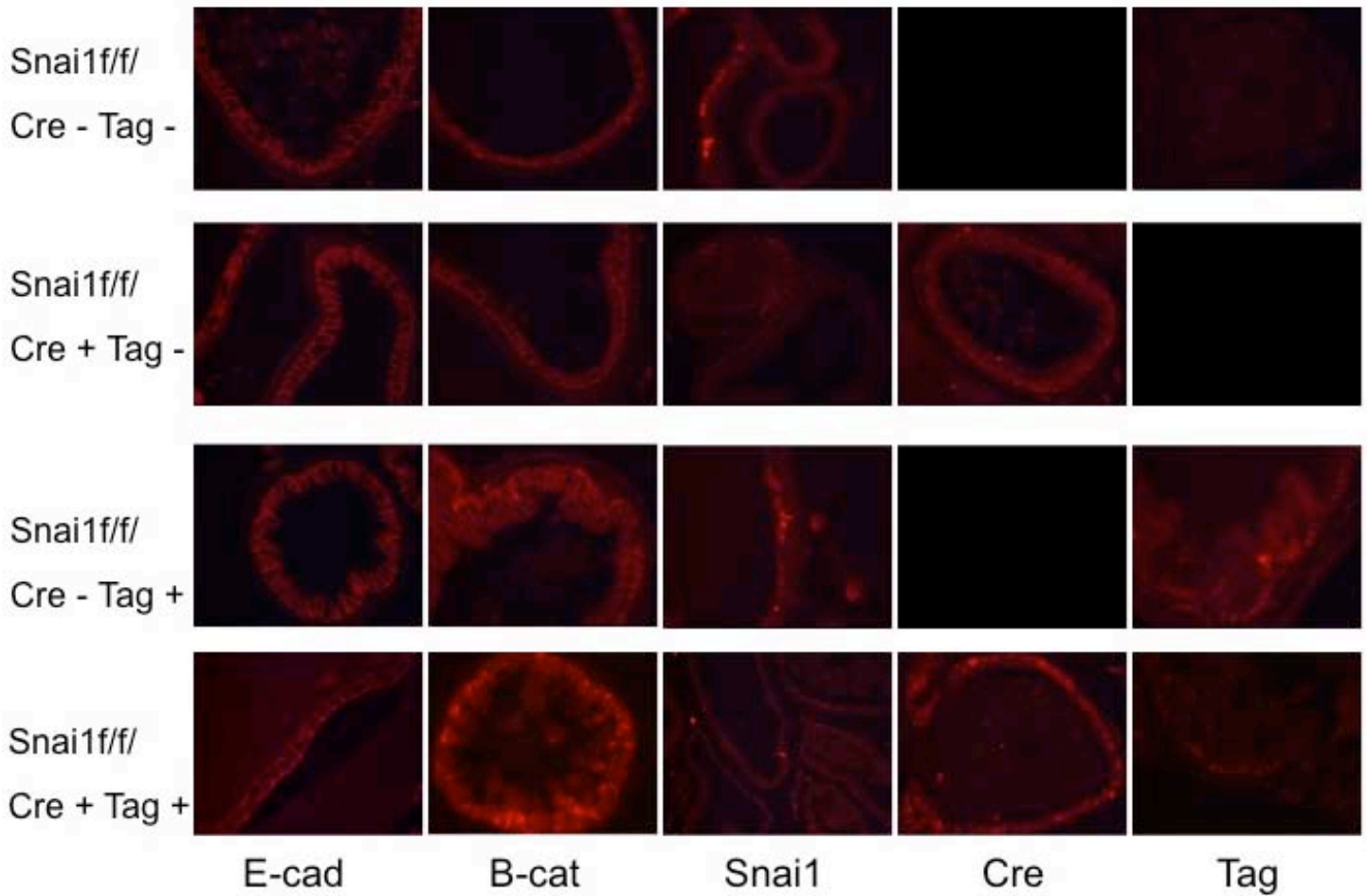
Beta-Actin	Forward 5' GTGGGCCCGCCCTAGGCACCAA Reverse 5' CTCTTTGATGTCACGCACGATTTC
Beta-Catenin	Forward 5' TGAAGGTGCTGTCTGTCTGC Reverse 5' GCTGCACTAGAGTCCCAAGG
Calponin	Forward 5' GCACATTTTAACCGAGGTCC Reverse 5' TGACCTTCTTCACAGAACCC
E-cadherin	Forward 5' GACAACGCTCCTGTCTTCAAC Reverse 5' TCTGTGACAACAACGAACTGC
GAPDH	Forward 5' CATGGCCTTCCGTGTTTCCTA Reverse 5' CCTGCTTACCACCTTCTTGAT
Snai1Flox	Forward 5' CGGGCTTAGGGTGTTCAGAA Reverse 5' CTTGCTTGGTACCTGCCTTC
Snai1 Flox Deletion	Reverse 5' TGAAAGCGGCTCTGTTCAGT
S16	Forward 5' AGGAGCGATTTGCTGGTGTGGA Reverse 5' GCTACCAGGCCTTTGAGATGGA
Snai1	Forward 5' CAACTATAGCGAGCTGCAGGA Reverse 5' ACTTGGGGTACCAGGAGAGAGT
Vimentin	Forward 5' GTTTCCAAGCCTGACCTCACTG Reverse 5' CTCTTCCATCTCACGCATCTGG
Wnt 3	Forward 5' AAATTGGGTAGCCAGCGAGGAC Reverse 5' ACTTCAGGGTGAGTTTGGGGAC
Zeb1	Forward 5' GGAAACCGCAAGTTCAAGTG Reverse 5' CACCACACCCTGAGGAGAAC

Figure 3. Hematoxylin and Eosin staining of Snai1 floxed mouse prostates.



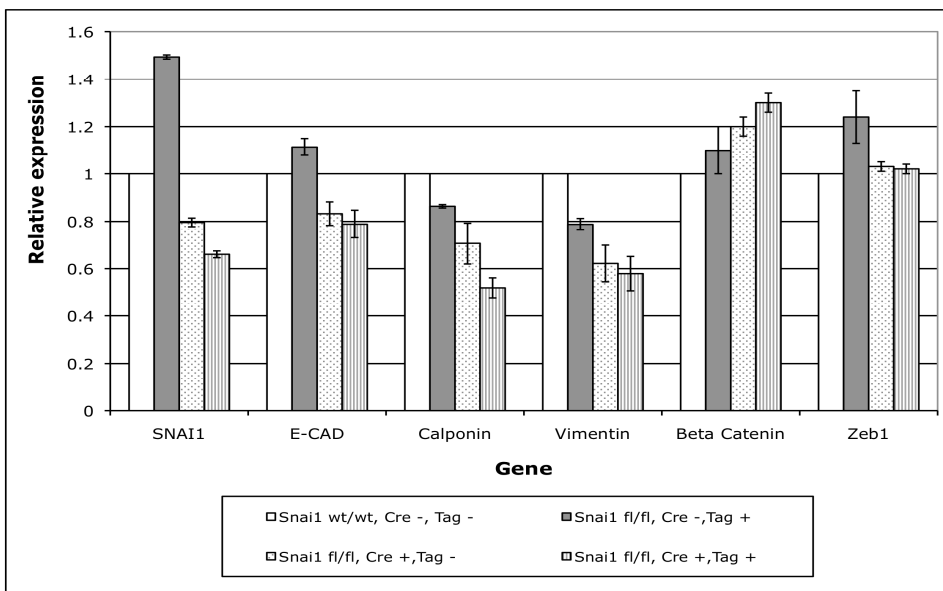
Sections of 30W mouse prostate lobes. We examined the each of the mouse prostate lobes and noticed severe morphological changes in Snai1f/f/ x PBCRE x TRAMP positive compared to Snai1f/f/ PBCRE negative TRAMP negative or TRAMP positive. Mice that are Snai1f/f/ PBCRE and TRAMP positive still have anterior (AP), dorsal (DP), lateral (LP) and ventral (VP) prostates which maintain their overall glandular form have disorganized epithelial cells.

Figure 4. Immunofluorescent staining of E-cadherin, Beta-catenin, Snai1, Cre and T-antigen (TRAMP) in Snai1f/f/ x PBCRE +/- x TRAMP +/- mouse ventral prostates



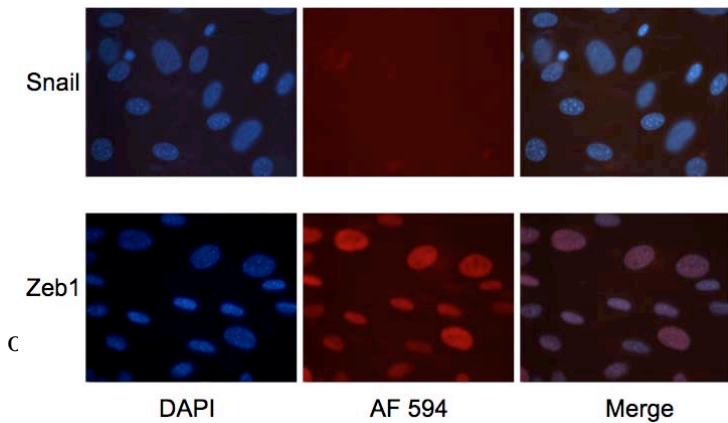
40X Immunofluorescent staining of E-cadherin, Beta-catenin, Snai1, Cre and Tag in Snai1f/f/ x PBCRE +/- x TRAMP +/- mouse prostate Ventral lobes. Staining of prostate lobes using specific antibodies and using a red fluorescent (594 nm) Alexa-Fluor secondary antibody for labeling.

Figure 5. Real-Time PCR analysis of gene expression in Snai1f/f/ x Cre +/- and TRAMP +/- mouse prostates



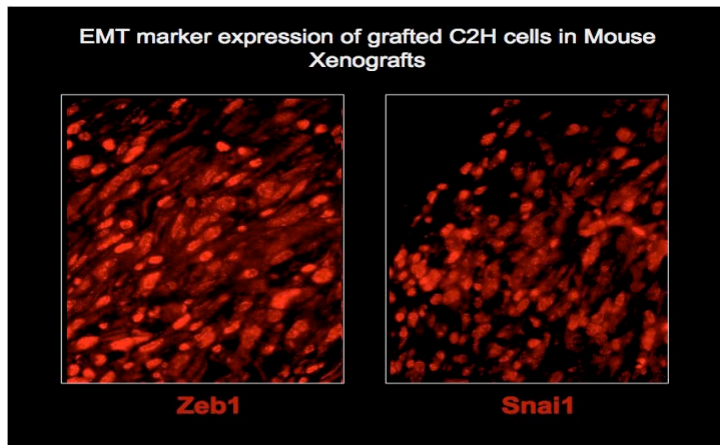
Real-Time PCR analysis of Snai1, E-cadherin, Calponin, Vimentin, Beta-Catenin and Zeb1 in Dorsal /Lateral mouse prostates (DLP). From 30W Snai1f/f/ x PBCRE +/- and TRAMP +/- whole mouse prostates. All samples were done in triplicate and all levels have been normalized to S16 and made relative to wild-type mouse prostates which was set to one.

Figure 6. Expression of Snai1 and Zeb1 in C2H cultured cells



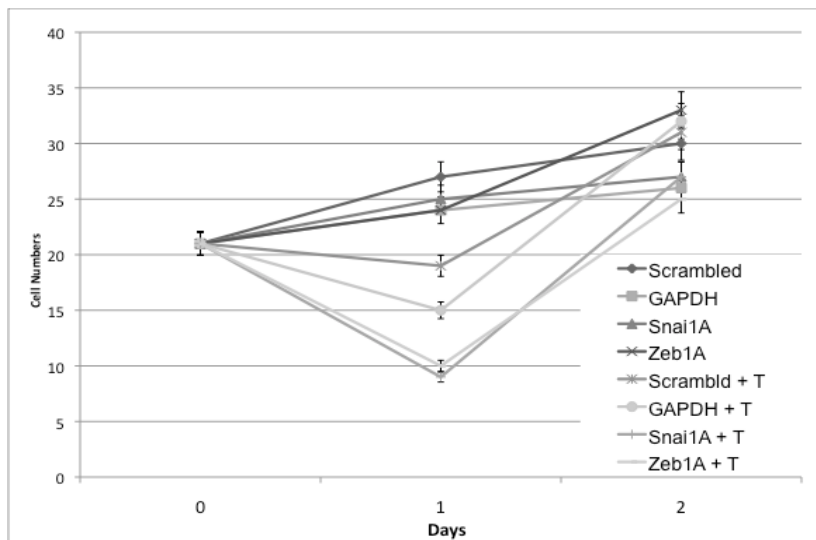
Immunohistochemical staining of cultured C2H cells. Formalin fixed cells were stained using antibodies to either Snai1 or Zeb1 and detected with a fluorescent red secondary antibody. DAPI dye was used to highlight cell nuclei. DAPI and red fluorescent images were merged together and shown the far right side.

Figure 7. Expression of Snai1 and Zeb1 in C2H cell NOD/SCID xenografts



Snai1 and Zeb1 staining of grafted C2H cells into NOD SCID mice. Xenografts were sectioned and stained with either Zeb1 or Snai1 primary antibody. A fluorescent red secondary antibody was used to detect the primary. Sections were then visualized and photographed under a fluorescent microscope.

Figure 8. Growth of C2H cells with shRNA knock-down of Snai1 or Zeb1



C2H cells were transfected with shRNA against Snai1 or Zeb1. These cells were then counted at 0, 24 and 48 hours after transfection. GAPDH and Scrambled shRNA were used as controls. Another group of cells, in addition to shRNA transfection were also treated with the androgen analogue R1881. Average cell numbers were obtained daily by counting several fields using a hemocytometer and trypan blue staining.